

Article

Preparation of Regular Cement Hydration Crystals and Ordered Microstructures by Doping GON and an Investigation into Its Compressive and Flexural Strengths

Shenghua Lv ^{1,*}, Jia Zhang ², Linlin Zhu ¹, Chunmao Jia ³ and Xiaoqian Luo ¹

¹ College of Bioresources Chemical and Materials Engineering, Shaanxi University of Science and Technology, Xi'an 710021, China; zhull@yahoo.com (L.Z.); Luoxiaoqian@yahoo.com (X.L.)

² College of Environment Science and Engineering, Shaanxi University of Science and Technology, Xi'an 710021, China; zhangjia201611@yahoo.com

³ College of Chemistry and Chemical Engineering, Shaanxi University of Science and Technology, Xi'an 710021, China; jiacm1205@yahoo.com

* Correspondence: lvsh@sust.edu.cn; Tel.: +86-029-8613-2651

Academic Editor: Helmut Cölfen

Received: 22 March 2017; Accepted: 2 June 2017; Published: 5 June 2017

Abstract: In this work, we found that by controlling the size of the graphene oxide nanosheets (GON) at 5–140 nm, 5–260 nm and 5–410 nm, respectively, we could prepare regular shaped cement hydration crystals with the shape of nano-needle-like, flower-like, and polyhedron-like crystals, respectively. Together, these crystals formed an ordered structure of cement composites on both the micro and macro levels, and the compressive and flexural strengths of the cement composites obviously increased when compared to the control samples. Our results indicated that the smallest structural unit of regular crystals was the nano-polyhedron-like crystals, which consisted of AFt, AFm, CH, and crystallization C–S–H, and could assemble into regular needle-like crystals, flower-like crystals, and polyhedron-like crystals, as well as an ordered structure on the micro and macro levels. Most of the C–S–H was transferred into a monoclinic system crystals and the remainder played the role of an adhesive in the forming process of regular crystals and structure. The cracks and holes in the cement composites disappeared by the self-repairing effect of the growing hydration crystal. The results indicate that ordered structural cement composites with defect-free structures and high strength can be prepared using GON with a suitable size range.

Keywords: graphene oxide nanosheets; hydration crystals; crystal growing; cement composites; microstructure

1. Introduction

Currently, the main problem with cement composites is that cement hydration products always have various and irregular shapes [1–3], resulting in the formation of a disordered structure with many cracks and holes, a deterioration of their performance, and a reduction of their durability [4–8]. The cement mainly consists of tricalcium silicate (C_3S , $3CaO \cdot SiO_2$), dicalcium silicate (C_2S , $2CaO \cdot SiO_2$), tricalcium aluminate (C_3A , $3CaO \cdot Al_2O_3$), tetracalciumaluminoferrite (C_4AF , $4CaO \cdot Al_2O_3 \cdot Fe_2O_3$), and gypsum ($CaSO_4 \cdot 2H_2O$). Cement can carry out complex hydration reactions with water, and produce complex products such as ettringite (AFt, $3CaO \cdot Al_2O_3 \cdot 3CaSO_4 \cdot 32H_2O$), monosulfate (AFm, $3CaO \cdot Al_2O_3 \cdot CaSO_4 \cdot 12H_2O$), calcium hydroxide (CH, $Ca(OH)_2$), and calcium silicate hydrate (C–S–H, $3CaO \cdot 2SiO_2 \cdot 3H_2O$) [9–12]. Together, the cement hydration products construct the cement matrix, and their shape and aggregation has a significant influence on the performance of the cement composites.

In general, the proportion of AFt, AFm, CH, and C–S–H in cement hydration products is approximately 7–12%, 2–4%, 20–30%, and 50–70%, respectively [13]. These cement hydration products have various shapes and randomly agglomerate. AFt, AFm, and CH are usually crystals and may exhibit needle-like, hexagonal cylinder, polyhedron-like, rod-like, sheet, and other structures. C–S–H was always thought to be an amorphous solid, but was found to have short fibrous sheets and dendritic fibrous products [13]. Therefore, the ability to control the formation of regular cement hydration products can solve these existing problems. In previous studies, we found that graphene oxide nanosheets (GON) [14–16] with special chemical groups could regulate the cement hydration products to form nano-needle-like, flower-like, and polyhedron-like crystals, which obviously improved the strength and toughness of the corresponding cement composites [17–20]. However, we also found that GON were difficult to mix evenly with the cement paste. Thus, it was difficult to form large-scale regular structures in the whole cement composite, which is essential for practical engineering applications of GON. In this paper, we show that large-scale ordered structural cement composites consisting of regular nano-needle-like, flower-like and polyhedron-like cement hydration crystals can be prepared by selecting GON with an appropriate size. Moreover, the formation process of regular cement hydration crystals and their ordered structures was elucidated based on the experimental results. We also demonstrate that cement composites with regular structures display a striking improvement in strength and toughness.

2. Materials and Methods

2.1. Preparation of Graphene Oxide Nanosheets (GON)

A three-necked flask was placed in an ice bath (5 °C), and 3 g of powdered graphite, 60 g of concentrated H₂SO₄, and 3 g of NaNO₃ were added and mixed well. Next, 12 g of KMnO₄ was slowly added to the contents of the flask over 15 min with stirring. The reaction temperature was kept at 5 °C for 1 h, then increased to 35 °C for 6 h. 200 mL of deionized water was added to the flask and heated to 70 °C, following which, 30 g of H₂O₂ was dripped into the flask over 30 min. The final product was purified by centrifugation, precipitation, and washing repeatedly with deionized water until the washing water had a pH of 7.0. The centrifugal pipe size was 100 mL × 4, the centrifugal rotational speed was 10,000 rpm, and the centrifugal time was 5 min. The aqueous graphite oxide was further treated with 1800 W ultrasonic for 50 min, 70min, and 90 min, respectively, to prepare the GON with different sizes for cement composites.

2.2. Preparation of Cement Composites

The cement composites were prepared by mixing Portland cement (P.O 42.5), standard sand, water, polycarbonate superplasticizer (PCs), and GON. The weight ratio of cement, sand, water, PCs and GON was 100:300:35:0.2:0.03. The test sample size was 40 mm × 40 mm × 160 mm.

The preparation procedure was as follows. Water, PCs and GON were mixed and then ultrasonically treated for 30 min to prepare the GON/PCs composites. Then GON/PCs composites were mixed with cement and sand under stirring for preparing cement composites. The cement composites were poured into a mold for preparing samples. After 24 h, the samples were removed from the mold and cured in water at 20 °C until testing. The cement composites without GON were named as Sample-0, and the cement composites doped GON with the size ranges of 5–140 nm, 5–260 nm, and 5–410 nm were named Sample-1, Sample-2, and Sample-3, respectively.

2.3. Test Methods

The chemical structure in GON were measured by Fourier-transform infrared spectroscopy (FTIR; EQUINOX-55, Bruker, Ettlingen, Germany), and X-ray photoelectron spectroscopy (XPS; XSAM 800, Kratos, Manchester, UK). The surface morphologies of GON were examined by atomic force microscopy (AFM; SPI3800N/SPA400, Seiko, Osaka, Japan), and laser particle analyzer (LPA,

NANO-ZS90, Zetasizer, Worcestershire, UK). X-ray diffraction (XRD; D/max2200PC, Rigaku, Osaka, Japan) used to examine the crystal phase structure in cement composites. The morphologies of the cement composites were determined by scanning electron microscope (SEM; S-4800, Hitachi, Tokyo, Japan). The composite samples were fixed to an aluminium stub and dried under an infrared lamp for 30 min, and coated with gold by a sputtering process.

The flexural strength was determined using a concrete three-point flexural strength tester (DKZ-500, Jianyi Instrument and Machinery, Co., Wuxi, China) at a pressure increase rate of 0.25 MPa/s. Compressive strength was tested with a compressive strength tester (JES-300, Jianyi Instrument and Machinery, Co., Wuxi, China) at a pressure increase rate of 1 MPa/s. The pore structure of the cement matrix was tested using an automatic mercury porosimeter (AutoPoreIV 9500, Micromeritics Co., Norcross, GA, USA). The dry samples were weighed accurately, placed in an expansion joint and sealed, subjected to low pressure (0–30 MPa), and then reweighed, and further tested at high pressure (30–400 MPa).

3. Results and Discussion

3.1. Structural Characterization of GON

The structural characterizations of the GON are shown in Figure 1. Figure 1a shows the FTIR spectra of the GON and was used to confirm the chemical groups present in the GON. The results indicated that the GON contained hydroxyl groups ($-\text{OH}$, 3350 cm^{-1}), carboxyl groups (COOH , 1740 cm^{-1}), carbonyl groups ($\text{C}=\text{O}$, 1660 cm^{-1}), and ether bonds ($-\text{C}-\text{O}-\text{C}-$, 1410 , 1260 , 1100 , 1050 cm^{-1}), which are not present on graphite. Figure 1b presents the XPS spectra of the GON and was used to determine the valence state of carbon, as well as the content of the chemical groups. The results indicated that the carbon bonds in the GON were $\text{C}=\text{C}$, $\text{C}-\text{OH}/\text{C}-\text{O}-\text{C}$, $\text{C}=\text{O}$, and COOH with contents of 3.49, 38.73, 46.40, and 11.38%, respectively. The size distribution of the GON in an aqueous solution is shown in Figure 1c, and the result indicates that the GON had size ranges between 5–140 nm, 5–260 nm, and 5–410 nm. Figure 1d shows an AFM image of the GON with a size range of 5–410 nm. The results indicate that the thickness of the GON was about 3.5 nm and had uneven surfaces.

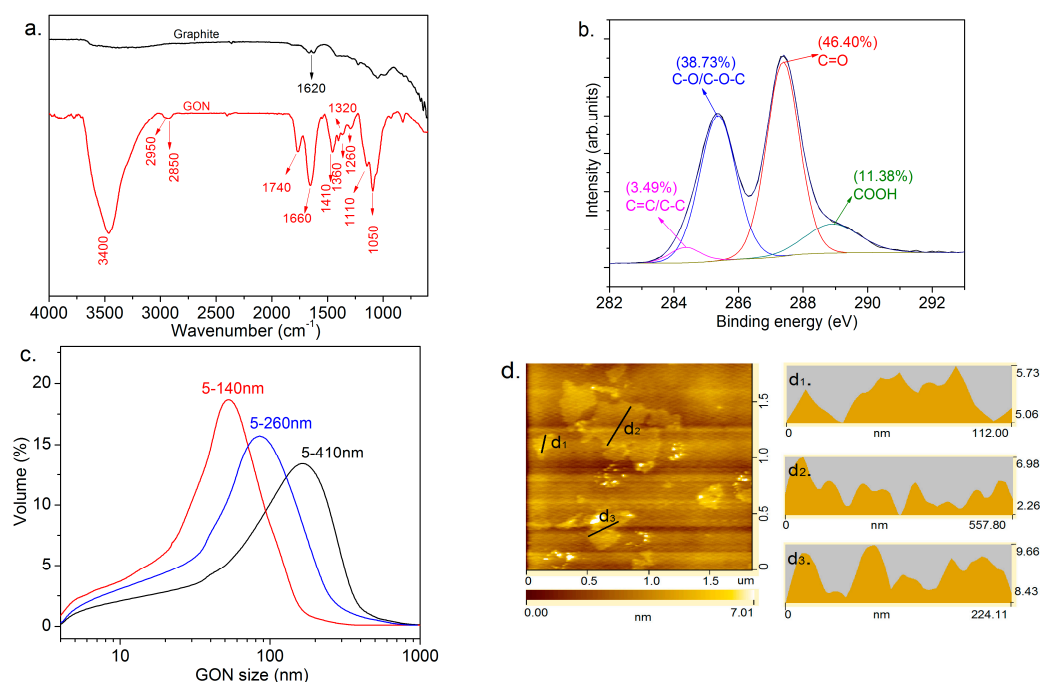


Figure 1. Structure characterization of GON. (a) FTIR spectra; (b) XPS spectra; (c) The size distributions; and (d) AFM images.

3.2. Microstructure Cement Composites

To determine the effect of the GON on cement composites, the microstructure of the cement composites without GON was investigated; the results are shown in Figure 2. The results show the SEM images of a cement matrix at 3, 7, and 28 days, respectively. The outstanding structural feature of the cement composites was the irregular microstructure and the existence of many cracks and large holes, as well as little needle-like and sheet-like crystals. Figure 2a,b show the microstructure at 3 days and 7 days, indicating that the cement hydration reaction was not fulfilled and that there existed many small hydration crystals and large holes. Figure 2c–f show the microstructure at 28 days, indicating that the cement hydration reaction was nearly complete and produced many needle-like and sheet-like crystals, as well as many large cracks. The main reason was due to the small amount of hydration crystals and their uneven distribution in the cement matrix, resulting in the production of many large cracks and serious decreases in strength and durability.

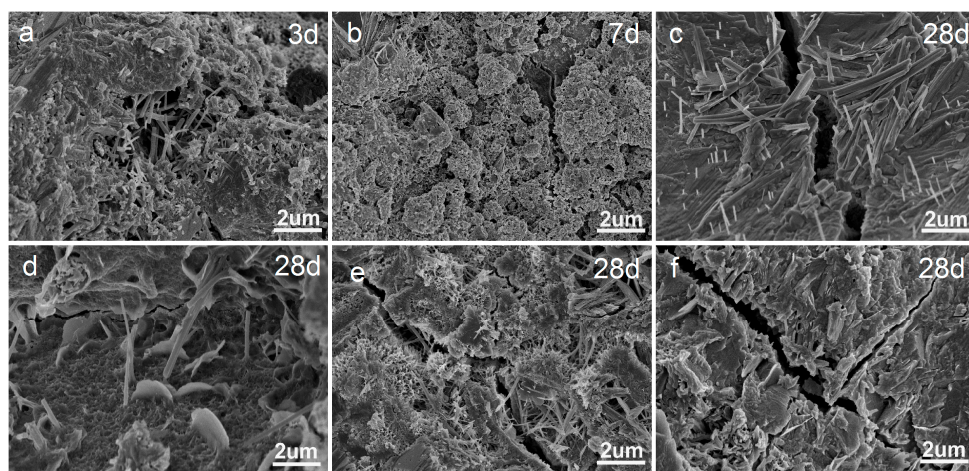


Figure 2. SEM images of cement composites without GON. (a) 3 days; (b) 7 days; (c–f) 28 days. The weight ratio of cement/sand/water/PCs was 100:300:35:0.2.

Figure 3 shows the microstructure of the cement composites doped with 0.03% of GON with a size range of 5–140 nm at 3, 7, and 28 days, named Sample-1. The images indicate that the cement hydration products were mostly regular nano-needle-like crystals and the microstructure was constructed through the crosslinking and agglomeration of nano-needle-like crystals. Figure 3a shows the microstructure at 3 days, and it was found that many regular nano-needle-like crystals had been produced which did not form acrosslinking structure. Figure 3b shows the microstructure at 7 days, indicating that the partial nano-needle-like crystals formed a compact structure by crosslinking and aggregation. Figure 3c–f show the microstructure at 28 days, indicating that the whole cement composite had formed a compact structure by interweaving of nano-needle-like crystals. The results confirm that the GON with a size range of 5–140 nm could control the formation of nano-needle-like crystals at an early stage, and then form a compact interweaving structure at a later stage of the curing process. The formation process exhibited self-assembly effects in the cement composites, which is beneficial for the formation of a compact and crosslinked network that produces a reinforced and toughened material.

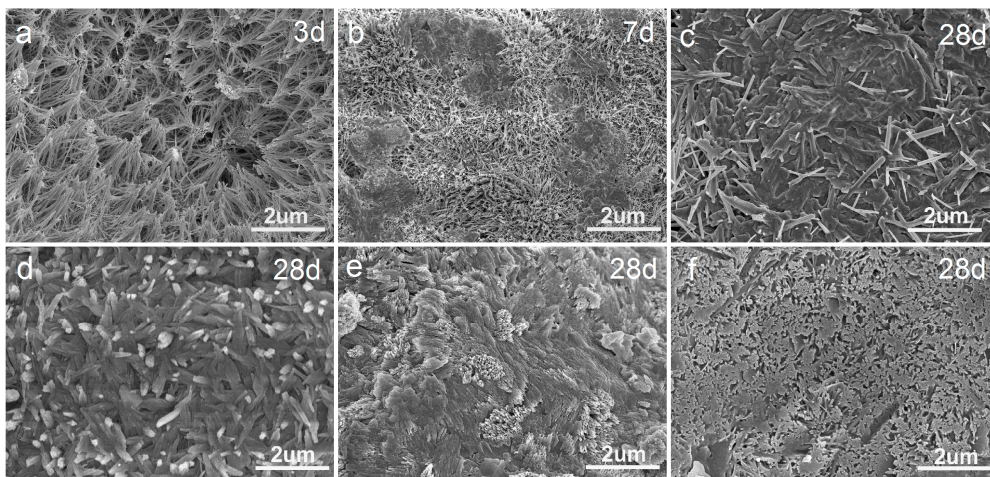


Figure 3. SEM images of Sample-1. (a) 3 days; (b) 7 days; (c–f) 28 days. The weight ratio of cement/sand/water/PCs/GON was 100:300:35:0.2:0.03.

Figure 4 shows the microstructure of the cement composites doped with 0.03% of GON with a size range of 5–260 nm cured for 3, 7, and 28 days, named Sample-2. A distinctive feature of the microstructure was that almost all the cement hydration products were controlled into rod-like crystals and assembled into flower-like patterns with GON. Figure 4a is the microstructure at 3 days, indicating many rod-like crystals were generated in the cement matrix and formed clusters of crystals with flower-like patterns, which could grow in the cement matrix. Figure 4b shows the aggregations of many flower-like crystals at 7 days, indicating that the crystals could grow with a tendency to form denser structures by the interweaving of nano-rod-like crystals. Figure 4c–f show several typical ordered structures of the cement composites under GON at 28 days, where the common structure feature was that the structure of cement composites was ordered with flower-like patterns and a completely compact microstructure was formed. The results indicated that GON with a size range of 5–260 nm could regulate the formation of flower-like crystals at an early stage from the interweaving network through crystal growth.

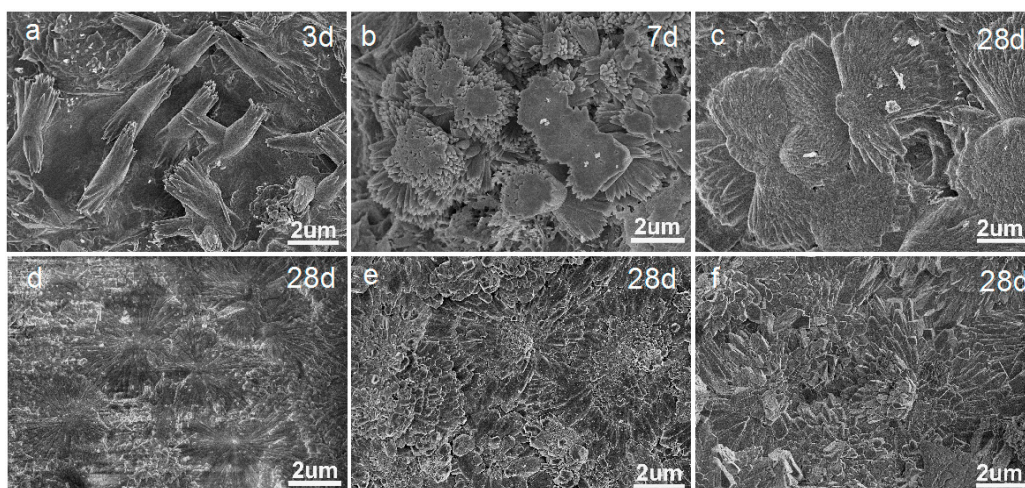


Figure 4. SEM images of Sample-2. (a) 3 days; (b) 7 days; and (c–f) 28 days. The weight ratio of cement/sand/water/PCs/GON was 100:300:35:0.2:0.03.

Figure 5 shows the microstructure of cement composites doped with 0.03% GON with a size range of 5–410 nm at 3, 7, and 28 days, named Sample-3. The results indicated that the cement matrix

was mostly composed of nano-polyhedron-like crystals. Figure 5a presents the microstructure of the cement composites at 3 days, showing that the cement matrix was mostly composed of nano-polyhedron-like crystals. Figure 5b shows the microstructure at 7 days, indicating that the cement matrix consisted of clusters of nano-polyhedron-like crystals. Figure 5c–f show the microstructure at 28 days, indicating that the cement composite formed perfect structures by the aggregation and crosslinking of the nano-polyhedron-like crystals. The results confirm that the GON with a size range of 5–410 nm could control the cement hydration products to form large-volume polyhedron-like crystals.

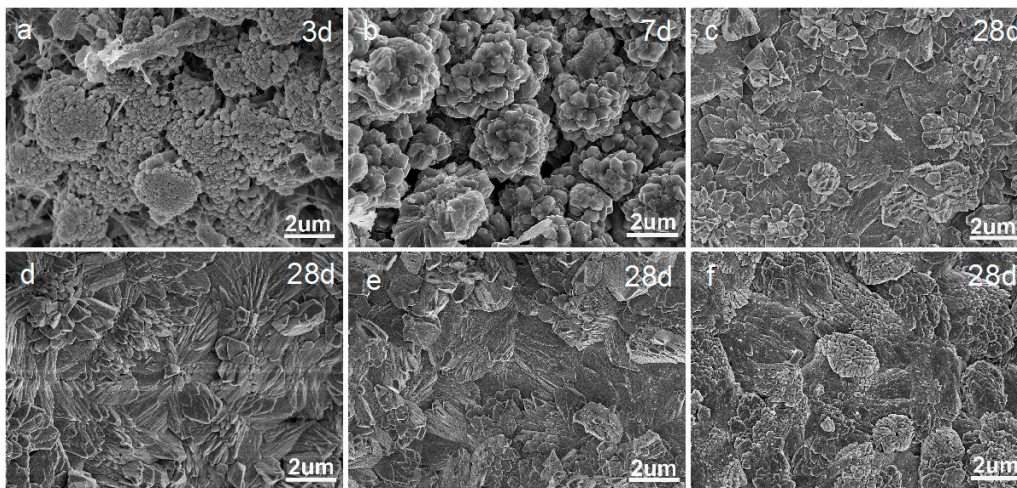


Figure 5. SEM images of Sample-3. (a) 3 days; (b) 7 days; and (c–f) 28 days. The weight ratio of cement/sand/water/PCs/GON was 100:300:35:0.2:0.03.

3.3. XRD Patterns Analysis and Compressive/Flexural Strengths of Cement Composites

Figure 6 shows the XRD patterns of the cement composites, indicating that there are many locations of crystalline peaks in the cement composites. Figure 6a shows the XRD pattern of cement composites without GON, indicating that the cement hydration crystals have an incomplete crystal phase structure. In particular, the C–S–H has a low crystalline structure, suggesting that it is almost all amorphous solid. Figure 6b shows the XRD pattern of cement composites with GON (Sample-3), indicating clearly that the crystal peaks are higher in comparison to Figure 6a. The results suggest that the cement hydration crystals have a complete crystal phase structure, and it was found that many crystalline peaks of C–S–H belong to monoclinic system crystals. The results suggest that C–S–H was transferred into regular crystals under the control of GON. Meanwhile, the XRD patterns of Sample-1 and Sample-2 were investigated and found to exhibit the same crystal phase as that in Figure 6b. Figure 6c shows the XRD patterns of Samples 0–3 in the same figure for comparison analysis. The results indicate that the crystalline peaks obviously increased from Sample-0 to -1, -2 and -3. The results suggest that the GON could not only control cement hydration to form regular crystals, but also could improve the degree of crystallization and make the whole cement matrix form a large-scale ordered structure. Importantly, most of C–S–H may be changed into regular crystals such as monoclinic system crystals, which together form regular crystals and an ordered structure. The remainder amorphous C–S–H acts as an adhesive, which can help form large-volume hydration crystals and ordered structure. Meanwhile, the results indicated that GON with the size range of 5–410 nm had stronger crystallization capacity when compared with GON with the size ranges of 5–140 nm and 5–260 nm. The cement composites doped with GON with the size range of 5–410 nm had perfect crystal structure.

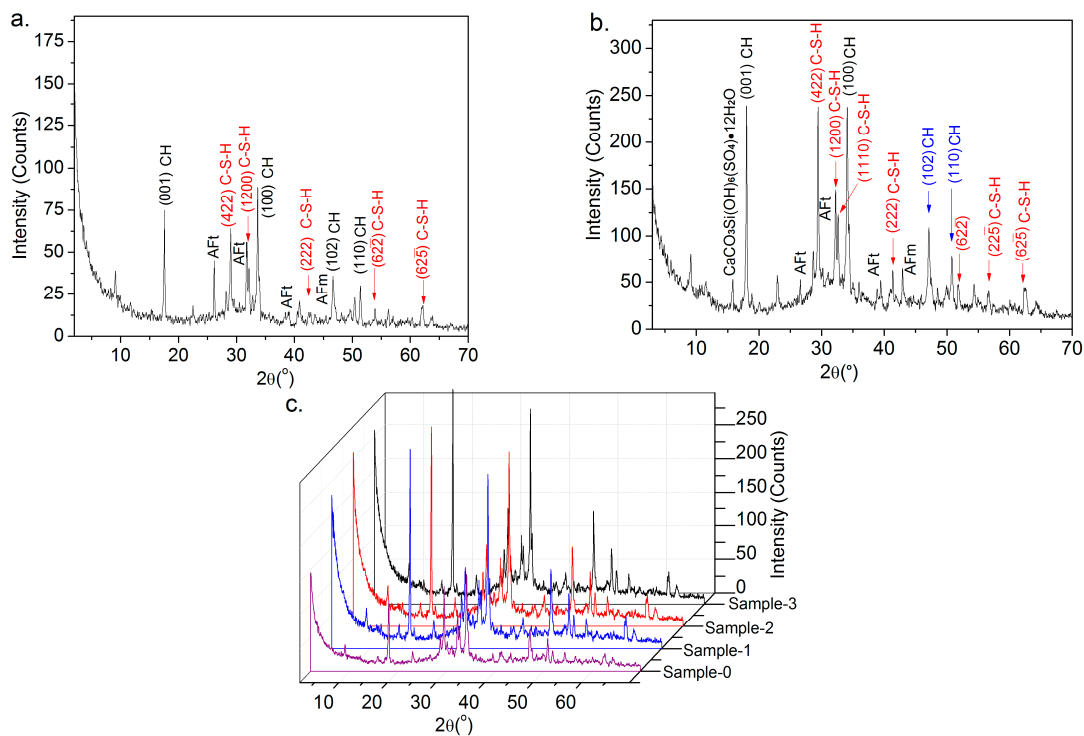


Figure 6. (a) XRD patterns of Sample-0 at 28 days; (b) XRD pattern of Sample-3 at 28 days; (c) XRD patterns of Sample 0–3 at 28 days.

Figure 7a shows the compressive strength of the cement composites at 28 days. The compressive strength of Sample-0, -1, -2, and -3 was 53.2, 84.4, 91.2, and 94.5 MPa, respectively. Compared with Sample-0, the increase ratio of Sample-1, -2, and -3 was 58.6%, 71.4%, and 77.6%, respectively. These results suggest that a cement composites with regular structure had an obvious reinforcing effect. Figure 7b is the flexural strength of the cement composites, indicating that the flexural strength of Sample-0, -1, -2, and -3 was 8.7, 15.3, 15.9, and 16.3 MPa, respectively. The increase ratio of flexural strength of the cement composites of Sample-1, -2, and -3 was 80.4%, 82.6%, and 88.5%, respectively. These results suggest that a regular microstructure had an obvious increased effect on flexural strength, and the increase ratio of flexural strength was greater than that of compressive strength. The results hint that the addition of GON in cement composites is very conducive to compressive and flexural strengths.

The pore structure of the cement composites was also investigated, and the results are shown in Figure 7c and Table 1. The results indicate the size range of GON has an important effect on the pore structure of the cement composites. The total pore area, pore size range, and average pore diameter of Sample-1, -2, and -3 are small compared with Sample-0, and the results indicate that the cement composites doped with GON have smaller average diameters compared with the cement composites without GON. The small size range of GON has a stronger capacity to decrease the pore diameter than the large size range of GON. The results suggest that GON, especially that with a large size, had significant impact on the shape and structure of the cement hydration crystals. One reason for this may be that a microstructure consisting of polyhedron-like and flower-like crystals has high compactness in comparison to needle-like crystals. The results indicated that GON with a large size can promote the formation of a regular microstructure with fewer cracks and holes. This explanation appears to be supported by the pore structure results and SEM images of the above mentioned cement composites.

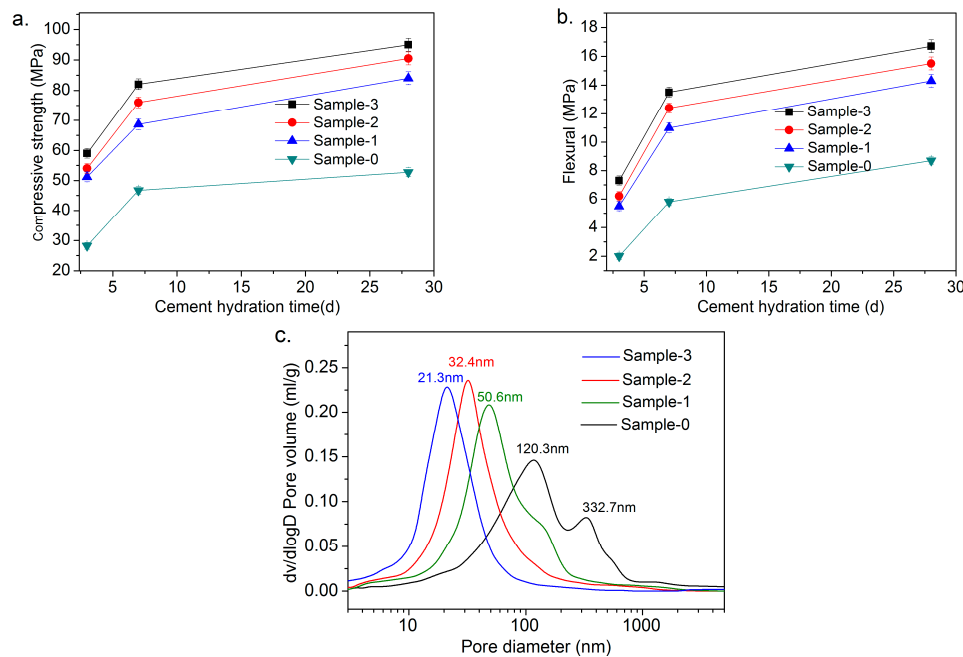


Figure 7. Strength and pore structure of Sample 0–3 at 28 days. (a) Compressive strengths; (b) Flexural strengths; and (c) Pore size distribution.

Table 1. Pore structure of the cement composites doped with GO at 28 days.

Samples	PDD (nm)	TPT (m ² /g)	MPD (nm)	APD (nm)	AD (g/cm ³)	Porosity (%)
Sample-0	20–800	21.12	226.55	180.51	2.4461	23.52
Sample-1	20–300	13.27	50.64	94.34	2.4623	12.83
Sample-2	10–150	9.46	32.42	42.35	2.4899	11.67
Sample-3	10–80	8.68	21.35	23.54	2.5311	10.54

PDD: pore diameter distribution; TPA: total pore area; MPD: mean pore diameter; APD: average pore diameter; AD: apparent density.

3.4. Formation Mechanism of Cement Hydration Products

In the study, we uncovered some interesting SEM images regarding cement hydration crystals that may help us understand the formation mechanism of cement hydration crystals under the control of GON. Figure 8a–c display the change process of the nano-needle-like crystals, indicating that the needle-like crystals can be assembled into flower-like crystals and polyhedron-like crystals. Figure 8d–f show another forming process of flower-like crystals, indicating that the large-volume flower-like crystals consisted mainly of smaller nano-polyhedron-like crystals. Figure 8g–i indicate the forming mechanism of large-volume polyhedron-like crystals, demonstrating that the nano-polyhedron-like crystals can be assembled into large-volume polyhedron-like crystals. These results also indicate that the needle-like, flower-like and polyhedron-like crystals could transform from each other by interweaving and assembly effects resulting in forming ordered structural cement composites in micro and macro level. Therefore, the formation mechanism was proposed in which GON plays a template effect to promote cement hydration to form as many needle-like and polyhedron-like crystals as possible, controlled by the size range of the GON. The small size of GON mainly controlled the cement hydration products to form nano-needle-like crystals and further developed a crosslinked network structure. The large size of GON mainly regulated the cement hydration products to form nano-polyhedron-like crystals and further produced large-volume flower-like and polyhedron-like crystals. The nano-needle-like and nano-polyhedron-like crystals, which consisted of AFt, AFm, CH and C–S–H, were considered the construction units forming the ordered structure on the macro and

micro levels. The regular cement hydration crystals produced at the initial hydration stage were further developed and inevitably resulted in the formation of regular structures by symbiosis, crosslinking, and interweaving. This process eventually formed regular cement hydration crystals and an ordered structure in whole cement composites.

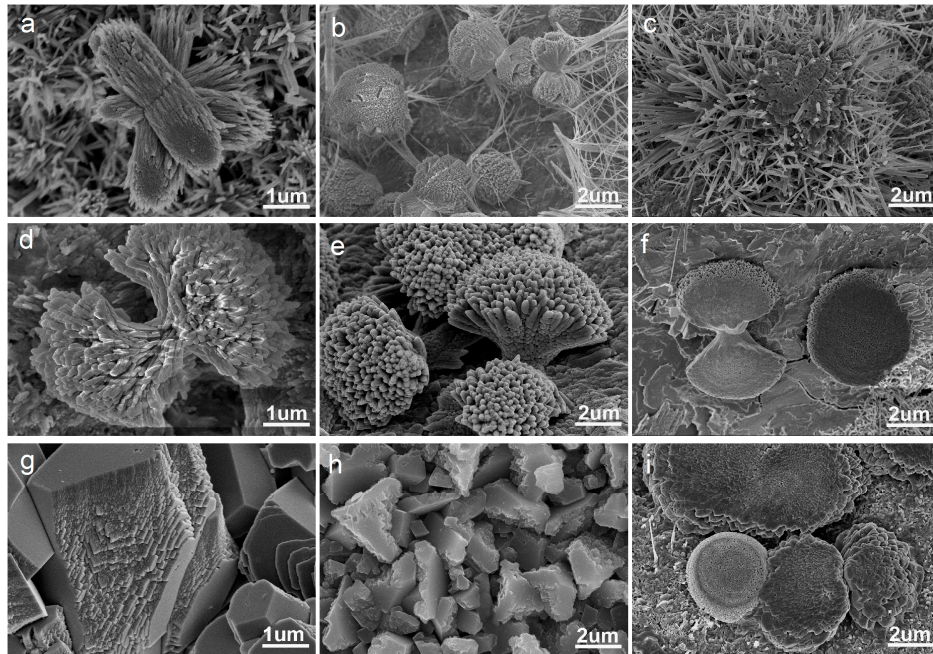


Figure 8. SEM images of cement composites doped with GON at 3 days. (a–c) Nano-needle-like crystals; (d–f) Flower-like crystals; (g–i) Polyhedron-like crystals.

4. Conclusions

GON can be used to control cement hydration products into regular nano-needle-like crystals by doping with GON in the size range of 5–140 nm, and nano-polyhedron-like crystals by doping with GON in the size ranges of 5–260 nm and 5–410 nm, respectively. These regular crystals can build an ordered microstructure through their symbiosis, crosslinking and interweaving, which is beneficial to the formation of an ordered structure with flower-like and polyhedron-like patterns to improve the compressive and flexural strengths of the cement composite.

The research results discovered that the smallest structure unit of regular crystals was nano-polyhedron-like crystals, which consisted of AFt, AFm, CH, and C–S–H, and could be assembled into regular needle-like crystals, flower-like crystals, and polyhedron-like crystals as well as an ordered structure on both the micro and macro levels. Most of C–S–H was transferred into regular crystals with monoclinic system crystals and the remainder acts as an adhesive in the formation process of regular crystals and structure. The cement hydration crystals were easier to grow in cracks and holes of the cement composites and had a tendency to form defect-free structures. The ordered structure is a kind of interpenetrating network by crosslinking, interweaving and symbiosis of needle-like, flower-like, and polyhedron-like crystals. The results show a great potential application in cement engineering.

Acknowledgments: The project was supported by the National Natural Science Foundation of China (21276152) and the Innovation Industrialization Foundation of Shaanxi Province of China (2016KTCL01-14).

Author Contributions: Shenghua Lv conceived of the research plan and wrote the paper. Jia Zhang, Linlin Zhu, Chunmao Jia and Xiaoqian Luo performed the experiments and analyzed the data.

Conflicts of Interest: The authors declare no conflicts of interest.

References

1. Di Bella, C.; Wyrzykowski, M.; Griffa, M. Application of microstructurally-designed mortars for studying early-age properties: Microstructure and mechanical properties. *Cem. Concr. Res.* **2015**, *78*, 234–244. [[CrossRef](#)]
2. Scrivener, K.L.; Juilland, P.; Monteiro, P.J.M. Advances in understanding hydration of Portland cement. *Cem. Concr. Res.* **2015**, *78*, 38–56. [[CrossRef](#)]
3. Bligh, M.W.; d'Eurydice, M.N.; Lloyd, R.R. Investigation of early hydration dynamics and microstructural development in ordinary Portland cement using ¹HNMR relaxometry and isothermal calorimetry. *Cem. Concr. Res.* **2016**, *83*, 131–139. [[CrossRef](#)]
4. Gdoutos, E.E.; Konsta-Gdoutos, M.S.; Danoglidis, P.A. Portland cement mortar nanocomposites at low carbon nanotube and carbon nanofiber content: A fracture mechanics experimental study. *Cem. Concr. Compos.* **2016**, *70*, 110–118. [[CrossRef](#)]
5. Ghatefar, A.; El-Salakawy, E.; Bassuoni, M.T. Early-age restrained shrinkage cracking of GFRP-RC bridge deck slabs: Effect of environmental conditions. *Cem. Concr. Compos.* **2015**, *64*, 62–73. [[CrossRef](#)]
6. Lameiras, R.; Barros, J.A.O.; Azenha, M. Influence of casting condition on the anisotropy of the fracture properties of Steel Fibre Reinforced Self-Compacting Concrete (SFRSCC). *Cem. Concr. Compos.* **2015**, *59*, 60–76. [[CrossRef](#)]
7. Wang, J.J.; Basheer, P.A.M.; Nanukuttan, S.V. Influence of service loading and the resulting micro-cracks on chloride resistance of concrete. *Constr. Build. Mater.* **2016**, *108*, 56–66. [[CrossRef](#)]
8. Shen, D.J.; Jiang, J.L.; Shen, J.X. Influence of curing temperature on autogenous shrinkage and cracking resistance of high-performance concrete at an early age. *Constr. Build. Mater.* **2016**, *103*, 67–76. [[CrossRef](#)]
9. Quercia, G.; Lazaro, A.; Geus, J.W.; Brouwers, H.J.H. Characterization of morphology and texture of several amorphous nano-silica particles used in concrete. *Cem. Concr. Compos.* **2013**, *44*, 77–92. [[CrossRef](#)]
10. Chakraborty, S.; Kundu, S.P.; Roy, A.; Adhikari, B.; Majumder, S.B. Effect of jute as fiber reinforcement controlling the hydration characteristics of cement matrix. *Ind. Eng. Chem. Res.* **2013**, *52*, 1252–1260. [[CrossRef](#)]
11. Ntalfalias, E.; Koutsoukos, P.G. Spontaneous precipitation of calcium silicate hydrate in aqueous solutions. *Cryst. Res. Technol.* **2010**, *45*, 39–47. [[CrossRef](#)]
12. Montagnino, D.; Costa, E.; Massaro, F.R.; Artioli, G.; Aquilano, D. Growth morphology of gypsum in the presence of copolymers. *Cryst. Res. Technol.* **2011**, *46*, 1010–1018. [[CrossRef](#)]
13. Bensted, J.; Barnes, P. *Structure and Performance of Cements*; Spon Press: London, UK, 2008.
14. Compton, O.C.; Nguyen, S.T. Graphene oxide, highly reduced graphene oxide, and graphene: Versatile building blocks for carbon-based materials. *Small* **2010**, *6*, 711–723. [[CrossRef](#)] [[PubMed](#)]
15. Yang, H.; Jiang, J.; Zhou, W.; Lai, L.; Xi, L.; Lam, Y.M.; Shen, Z.; Bahareh, K.; Yu, T. Influences of graphene oxide support on the electrochemical performances of graphene oxide–MnO₂ nanocomposites. *Nanoscale Res. Lett.* **2011**, *6*, 1–8. [[CrossRef](#)] [[PubMed](#)]
16. Gil, G.A.; Sandra, M.A.; Cruz, A.; Ramalho, J.G.; Marques, A.A.P. Graphene oxide versus functionalized carbon nanotubes as a reinforcing agent in a PMMA/HA bone cement. *Nanoscale* **2012**, *4*, 2937–2945.
17. Lv, S.H.; Ma, Y.J.; Qiu, C.C.; Sun, T.; Liu, J.J.; Zhou, Q.F. Effect of graphene oxide nanosheets on microstructure and mechanical properties of cement composites. *Constr. Build. Mater.* **2013**, *49*, 121–127. [[CrossRef](#)]
18. Lv, S.H.; Liu, J.J.; Sun, T.; Ma, Y.J.; Zhou, Q.F. Effect of GO nanosheets on shapes of cement hydration crystals and their formation process. *Constr. Build. Mater.* **2014**, *64*, 231–239. [[CrossRef](#)]
19. Lv, S.H.; Sun, T.; Liu, J.J.; Zhou, Q.F. Use of graphene oxide nanosheets to regulate the microstructure of hardened cement paste to increase its strength and toughness. *CrystEngComm* **2014**, *16*, 8508–8516. [[CrossRef](#)]
20. Lv, S.H.; Deng, L.J.; Yang, W.Q.; Zhou, Q.F.; Cui, Y.Y. Fabrication of polycarboxylate/graphene oxide nanosheet composites using copolymerization, for reinforcing and toughening cement composites. *Cem. Concr. Compos.* **2016**, *66*, 1–9. [[CrossRef](#)]

